

BEAM TRANSPORT AND SPECIAL UNDULATORS DESIGNED FOR HIGH POWER FELS*

Yu.P. Bouzouloukov, O. V. Chubar, A.S. Khlebnikov, N.S. Osmanov, A.V. Smirnov,
S.V. Tolmachev, A. Tulupov,
Russian Research Center "Kurchatov Institute", Moscow 123182, Russia
M. Caplan,
Lawrence Livermore National Laboratory, Livermore, CA 94550 USA

Abstract

One of the most important problem in designing of FELs for plasma fusion is optimizing of e-beam transport. High-average-power of the sectioned FEMs with beam recovering and high efficiency impose a stringent limit on e-beam losses as little as 0.2%. The approach considered here for two-section undulator designs contains i) optimum focusing strengths option and e.b. matching; ii) transport simulations with taking into account non-linear transverse space charge forces; iii) beam transport simulations in real undulators in terms of measured quasi-3D field data updated in the code.

1. INTRODUCTION

In designing of sectioned high power FEMs with beam recovering the following specific problems of beam transport to be solved: optimum focusing strength option and transport simulation with taking into account transverse space charge forces. Three variants for 5MW conceptual FEM designs were considered:

Table 1. Parameters used in simulations
Electron beam

Variant number	1	2	3
Emittance $\varepsilon_{nx,y}$, π mm mrad	50	80	50
Current I, A	30	30	20
Kinetic energy E , MeV	2.0	1.75	2.4
Beam radius, mm	1.2	1.2, 1.4	0.8
Perveance $S_{x,y}$	0.13	0.08	0.07

Two-section undulator

Variant	1	2	3
Period λ_w , cm	4	4	5
Field $B_{\nu 0}$, kGs	2.0; 1.6	2.0; 1.5	2.45; 2.2
Section lengths, cm	88; 64	76; 60	90; 80
Intersection gap, cm	6	6	7.5

The only difference between the first variant and FOM-FEM project [1] is the increased value of beam current. The second and third variants of undulator structure is a previous result of step-tapered high-gain FEM simulations using the 3D model [2].

The generalized perveance S is the scaling factor for estimation of space charge effect on transverse motion: $S_{x,y} = \pi \beta_{x,y} c / (\gamma^2 v_z \varepsilon_{nx,y} I_A)$, where $\beta_{x,y} = I/k\beta_{x,y}$ are the beam beta-functions, $I_A = mc^3/e$ and v_z is the beam longitudinal velocity. Since S is comparable with unity and intersection gap can increase space charge influence the transverse space charge effect should be taken into account in beam transport simulations.

2. RELATIVE FOCUSING STRENGTH OPTIMIZATION

Preliminary calculations determined the optimal focusing strengths on the basis of modified Kapchinskij-Vladimirskij equations [3]. These equations can be applied when the paraxial $(k_x r_{x,y})^2 \ll 1$ and smooth $\lambda_w k_{\beta_x, \beta_y} \ll 1$ approximations are satisfied, where $k_x^2 + k_y^2 = k_w^2$. Matched e-beam input conditions depending on S can be applied automatically in this code for any focusing conditions within the framework of the theory [3]:

$$\beta_{bx,by} = \beta_{x,y} (S_{x,y} + \sqrt{1 + S_{x,y}^2}), \alpha_{xb,yb} = 0.$$

Here β_{bx}, β_{by} are the beam Twiss parameters, and $\varepsilon_{nx,y}$ are the transverse normalized emittances.

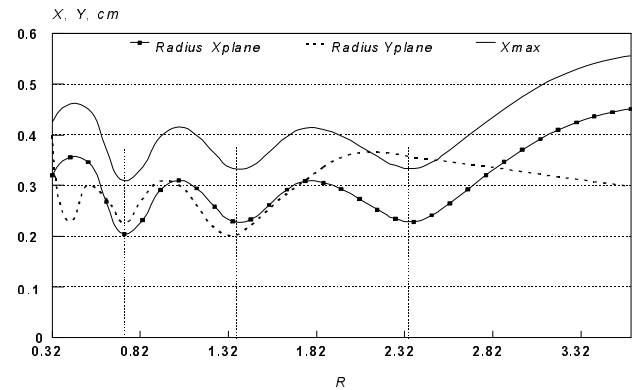


Figure 1. Beam confinement area as a function of relative focusing strength $R = k_{\beta_y} / k_{\beta_x}$ for the variant 2. To describe focusing properties when a superposition of the quadrupole and the periodic sextupole type fields

* This work is supported by Lawrence Livermore National Laboratory through Material Support Agreement No B 319818.

is used at negligible contribution of higher undulator harmonics, we introduced the following generalized expression of the relative focusing strength:

$$(k_{\beta_y} / k_{\beta_x})^2 = \frac{(K_w k_w / \beta_{\parallel} \gamma)^2}{Q e / \beta_{\parallel} \gamma m c^2 + (K_w k_x / \beta_{\parallel} \gamma)^2} - 1$$

Here K_w is the r.m.s. undulator strength, $k_w = 2\pi/\lambda_w$, $Q = -dB_y/dx$ and $\beta_{\parallel} = v_z/c$.

An example of beam occupied area as a function of relative focusing strength $R = k_{\beta_y}/k_{\beta_x}$ is depicted in Fig. 1

3. SOME RESULTS OF UNDULATOR MAGNETIC FIELDS MEASUREMENTS

Adjustable undulator structure with side magnets [4] was designed and investigated. High flexibility of the configuration is due to simultaneous variation of sextupole and quadrupole magnetic field components when the side magnets position changes.

Quasi-3D magnetic fields were measured for the variants 1,2 on full-scale undulator and for the variant 3 on the mock-up. A set of data containing gradients Q and field eigenvalues $k_{x,y}^2$ for each optimum (see Fig. 1) was extracted from the field map for all three variants. Focusing properties obtained from the processed measurement data are presented in ref. [5] for the first variant and in the Figs. 2,3 for second variant.

A common property of these plots is a monotonous dependency of gradient (growth, Fig. 2) and relative focusing strength (decrease, Fig. 3) versus side magnets shift.

Undulator field errors resulted in r.m.s. deviation of the relative focusing strength that lies within the range 0.06-0.17.

Longitudinal undulator wavenumber calculated from undulator field $B_{we}(0,0,z)$ measurements as $k_w^2 = \frac{1}{B_{we}^2} \frac{\partial^2 B_{we}}{\partial z^2}$ instead of $k_w = 2\pi/\lambda_w$ can be also an

important characteristic of undulator accuracy and focusing properties. Along with relation $k_x^2(z) + k_y^2(z) = k_w^2(z)$ such an approach is valid for paraxial approximation of the following kind:

$$\left| \frac{\partial k_x}{\partial z} x + \frac{\partial k_y}{\partial z} y \right| \ll |k_w|. \text{ Demonstrated in the Fig. 4}$$

behaviour of the $k_w^2(z)$ function was taken into account in the beam transport simulations in real undulator fields.

4. NON-AVERAGED BEAM TRANSPORT SIMULATIONS

The next step foresees more accurate multi-particle simulations done for the optimal values of relative focusing strengths found above. Transverse space charge forces using particle-mesh method, non-linear components of undulator non-averaged fields [6] and

different kinds of particle distribution were taken into account [7].

Non-linear components of focusing and space charge forces as well as coupling between transverse motion in XOZ and YOZ planes [8] resulted in differences of the beam envelopes behavior (compared with the linear model) that are most noticeable in the second section.

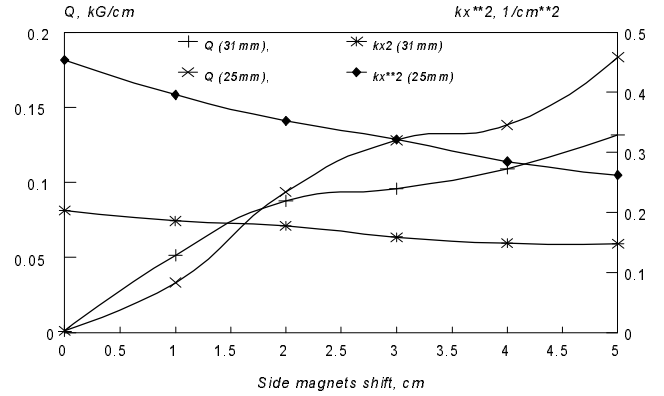


Figure 2. Gradient Q and sextupole parameter $k_x^2 = (\partial^2 B_y / \partial x^2) / B_{y0}$ as a function of side magnets displacement for the third variant and different horizontal distance between side magnets arrays.

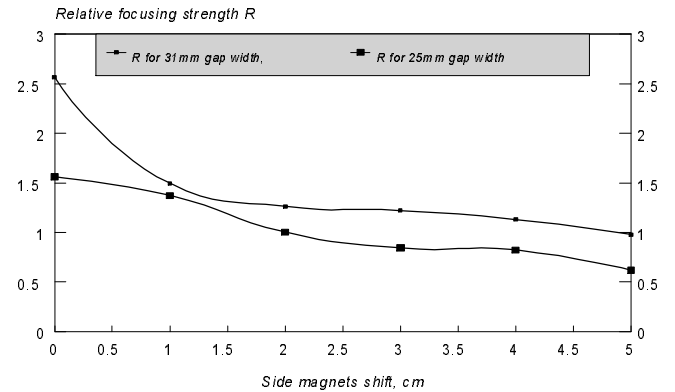


Figure 3. Relative focusing strength versus side magnets displacement for the third variant and different horizontal distance between side magnets arrays. $E = 2.4$ MeV.

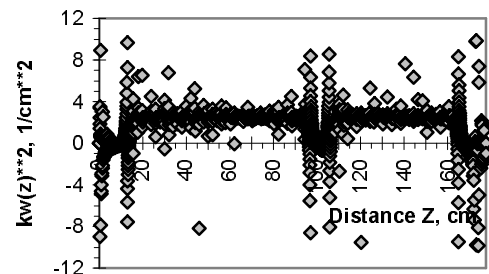


Figure 4. Longitudinal wavenumber squared k_w^2 [cm⁻²] plotted along the real undulator for the first variant.

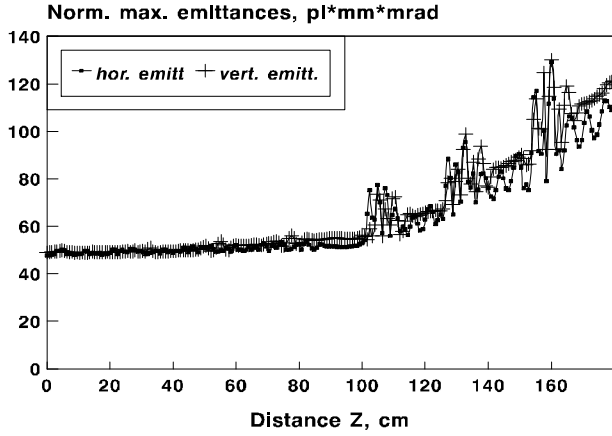


Figure 5. Beam edge emittances calculated for the third variant. Ideal focusing $k_y/k_x = k_{\beta y}/k_{\beta x} = 1$, $Q=0$.

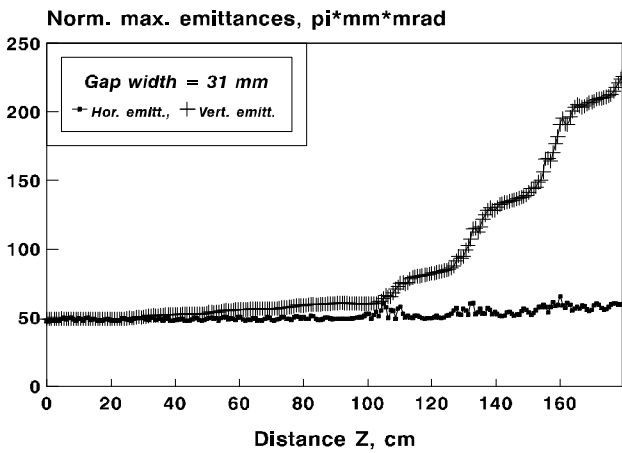


Figure 6. Beam r.m.s. emittances calculated for the third variant. Combined focusing, $k_{\beta y}/k_{\beta x} = 1$ corresponds to the gap width 31mm. Gaussian distribution, 8000 particles.

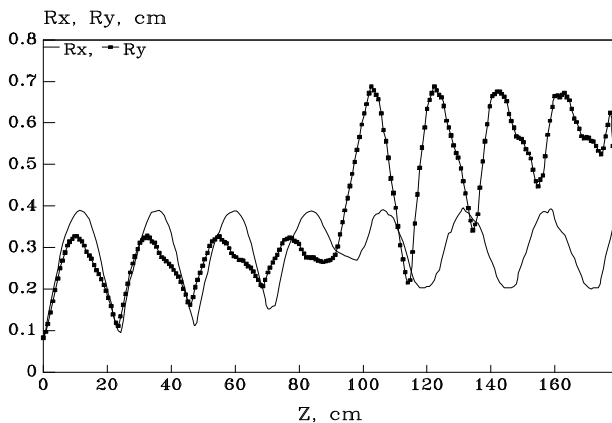


Figure 7. Beam edge envelopes calculated for the 3-rd variant. $k_{\beta y}/k_{\beta x} = 1$, the gap width 31mm, i.e. $Q=0.13$, 0.1 kG/cm, $k_x^2 = 0.15, 0.17$ cm⁻² cm⁻² in the first and second section. Input r.m.s. emittances are $\epsilon_{m,y} = 23 \pi$ mm mrad. Gaussian distribution, 3 particles from 8000 were lost on the upper and down walls of the waveguide.

Figs. 5,6 illustrate that ideal symmetric focusing ($R=1$, $Q=0$) and real combined focusing ($R=1$, $Q \neq 0$) gives rise to different emittance behavior. Two-section

undulator acceptance was estimated in terms of e.b. transport simulation at Gaussian distribution in transverse phase space (see Fig. 7).

5. CONCLUSION

1. Beam matching with the only first section is not optimal for the entire two-section due to intersection mismatching and beam space charge influence on the beam transport.
2. Non-perfect beam matching between undulator sections causes edge emittance growth. The main contribution in this growth gives beam interaction with the sextupole component. Hence the beam propagation can be slightly asymmetric in undulator even with perfectly symmetric focusing ($R=1$) but having $Q \neq 0$. Another reason of asymmetry is violation of the condition $R=1$ at the sections edges at combined focusing.
3. Beam propagation at $R > 1$ can be more stable to fields errors compared with equal focusing $R=1$.
4. Calculated acceptance of the system undulator + waveguide is 358π mm mrad (variant 3).

6. REFERENCES

- [1] W.H. Urbanus, W.A. Bongers, G. van Dijk, C.A.J. van der Geer, A.G.R.J.E. van Honk, P. Manintveld, A.B.Sterk, M. Valentini, A.G.A. Verhoeven, R.M.M. Weijman, M.J. van der Wiel, A.A.Varfolomeev, S.N. Ivanchenkov, A.S. Khlebnikov, M. Caplan, L. Bratman, G. Denisov. Construction, Testing of the 1 MW, 130-260 GHz Fusion-FEM, - presented at the 16-th Int. FEL Conf. and to be published in NIM A (1996).
- [2] M.Caplan, T. Antonsen, B. Levush, A. Tulupov and W. Urbanus, Nucl. Instrum. and Meth., A 358 (1995) 174
- [3] I.M. Kapchinskij, The Theory of Linear Resonance Accelerators. Moscow, Energoizdat, 1982 (in Russian).
- [4] W.H. Urbanus, R.W.B. Best, A.G.A. Verhoeven, M.J. van der Wiel, M. Caplan, L. Bratman, G. Denisov, A.A.Varfolomeev and A.S. Khlebnikov. Nucl. Instrum. and Meth., NIM A 331 (1993) 235.
- [5] A.A. Varfolomeev, Yu.P. Bouzouloukov, S.N. Ivanchenkov, A.S. Khlebnikov, N.S. Osmanov, M.J. van der Wiel, W.H. Urbanus, Nucl. Instrum. and Meth., NIM A 358 (1995) 396.
- [6] A.V. Smirnov, Nucl. Instrum. and Meth., A349, 295 (1994)
- [7] A.V. Smirnov. Preprint IAE-5655/14, Moscow, Russia (1993)
- [8] J.J. Barnard. Nucl. Instr. and Meth. A296(1990) 508.